UDC 004.932:616-073.756.8
DOI: 10.15587/2706-5448.2026.352787

Svitlana Alkhimova,
Viktoriia Sorokina,
Illia Kabala

COMPARATIVE ASSESSMENT OF COMMONLY USED COLOR LOOKUP TABLES TO DETERMINE KEY PERFORMANCE INDICATORS FOR PERFUSION MAP DATA VISUALIZATION

The object of this research is color lookup table schemes that are most commonly used to visualize perfusion maps in the scope of assessment of brain hemodynamic parameters. The problem is that such color schemes differ significantly in the number of colors, their distribution, and the rules for converting grayscale image data into color. As a result, the same perfusion map may appear different depending on the selected scheme, which complicates the visual assessment of hemodynamic parameters and significantly biases the precision of their interpretation.

The research provides a comprehensive analysis of the ten commonly used color lookup table schemes for perfusion map visualization. Assessment of both direct schemes and patient-derived data is provided. Among quantitative metrics are RMSE, PSNR, SSIM, FSIM, ISSM, SRE, SAM, and UIQ. The CIELAB color space is used to provide a perceptual assessment of the color impact across neighboring levels in the schemes. It also used to analyze the relationship between local intensity differences in greyscale perfusion maps and resulting color perceptual differences once the lookup table is applied. Analysis reveals that the selection of color lookup table schemes is critical for preserving signal intensity and structural integrity. Spectral rainbow and block-structured schemes lag behind others in performance, making them less effective due to distorted structural features.

The results can be applied in practice to visualize perfusion map data in medical software to assess key hemodynamic parameters, such as blood volume, blood flow, and mean transit time. Also, the results can be helpful for standardization and selecting optimal color lookup table schemes in clinical practice, and for validating algorithms used to calculate perfusion maps during medical software development.

Keywords: *colormap, color perception, color visualization, hemodynamic parameters, perfusion-weighted images.*

Received: 22.11.2025
Received in revised form: 28.01.2026
Accepted: 20.02.2026
Published: 28.02.2026

© The Author(s) 2026
This is an open access article under the Creative Commons CC BY license
https://creativecommons.org/licenses/by/4.0/

How to cite
Alkhimova, S., Sorokina, V., Kabala, I. (2026). Comparative assessment of commonly used color lookup tables to determine key performance indicators for perfusion map data visualization. Technology Audit and Production Reserves, 1 (2 (87)), 85–92. https://doi.org/10.15587/2706-5448.2026.352787

1. Introduction

In medical diagnostics, clinicians frequently base their treatment decisions on the medical image data. Typically, the end-point step of medical imaging workflow involves analysis of such data through advanced visualization techniques. Consequently, the effective visualization of data derived from various medical imaging methods is essential for improving diagnostic precision and supporting better-informed clinical decision-making.

Perfusion is the passage of fluid through the lymphatic system or blood vessels to an organ or tissue [1]. Dynamic susceptibility contrast magnetic resonance imaging (DSC-MRI) is a technique that creates perfusion-weighted images (PWI) using a T2-weighted MRI sequence [2]. These images are obtained when a contrast agent passes through the vascular system of scanned tissues. The contrast agent's susceptibility reduces the signal intensity on T2-weighted images. This signal change over time is transformed into time-concentration curves, which are the basis for perfusion analysis. It is provided pixel-by-pixel by deconvolving an arterial input function and tissue time-concentration curve, which is often implemented using singular value decomposition deconvolution methods [3]. The output of perfusion analysis consists of quantitative hemodynamic parameter values and associated perfusion maps, which provide a visual interpretation of the data. The key hemodynamic parameters commonly quantified are blood volume (BV), blood flow (BF), and mean transit time (MTT).

Perfusion map data are usually real numbers and can therefore be visualized as grayscale images [4]. To improve visual perception and data interpretation, these maps are converted from grayscale to color using color lookup tables (LUTs) [5], which are pre-calculated reference tables that map input values to output values. Briefly speaking, LUT is used to quickly convert color data from one set of values to another.

As effective visualization plays a crucial role in medical diagnostics, color LUT schemes are widely used to represent medical images [6, 7]. In the case of perfusion analysis, color LUT schemes are used to improve the interpretation of perfusion map data so that physicians can quickly assess a patient's condition (e. g., if a perfusion map shows blood flow in the brain, the color coding of the map can help identify areas with abnormally low or high values of this hemodynamic parameter).

The main components of the LUT scheme are the initial scale of values. This scale of values is a set of numbers representing the intensity

ISSN-L 2664-9969; E-ISSN 2706-5448

or quantitative indicators of the output data, and the color scale, which is a set of colors corresponding to these numbers. Each LUT scheme differs in the number of colors and the rules for applying them when converting a grayscale image to a color image. Consequently, the usage of different LUTs produces various effects on the interpreter's perception [8].

Well-known color LUT schemes, such as *Jet* or *Rainbow*, can present visual distortion that may lead to misinterpretation of scientific results, as they do not uniformly represent data ranges in continuous or binned variables [9–12]. Despite that, such schemes continue to be used in scientific literature [13]. After surveying 997 scientific publications in three different journals, the authors found that approximately 24% of papers use *Rainbow* color LUT scheme. They noted a 99.6% chance that a reader would encounter at least one visually problematic figure in a random sample of 10 papers.

As shown in recent studies, poor selection of color LUTs can result in information loss or misinterpretation of structures, especially when using schemes with nonlinear color changes [14, 15]. In light of this, a color LUT scheme is considered optimal if the distances between adjacent colors in the perceptual space are approximately equal. Lack of perceptual uniformity can create false visual contrasts that do not actually exist in the data. When applied to medical images, it can affect the detection of subtle details, specifically in the context of identifying pathological areas [16]. Significant limitations of studies mentioned above, however, are that they relied on subjective user trials and focused solely on basic perceptual distance measurements between colors within the colormap.

To address the challenges faced by viewers with color vision deficiency, several optimized color LUT schemes were proposed to ensure that data remains interpretable by linearizing color distances [17]. However, these schemes were derived from idealized mathematical models that may not reflect the complex, modality-specific structures in clinical medical images.

The effectiveness of colormaps that are perceptually uniform can vary depending on spatial frequency, since the human eye relies more on luminance than on chromaticity to detect small details [18]. To examine how effectively different colormaps allow users to detect small features in data, the authors utilized sinusoidal patterns to measure detection thresholds. While such patterns are assumed to be representative in vision science, they do not reflect the complex, irregular shapes and structures typically found in clinical data, such as medical images.

In the case of perfusion maps, they are also often visualized using different color LUT schemes with varying numbers of colors and construction principles. The choice of color LUT scheme may depend on the particular hemodynamic parameters, the capabilities of the medical software used, and even the physician's prior experience and preferences. As a result, the selected schemes may complicate the visual assessment of hemodynamic parameters and affect the precision of their interpretation, leading to wrong clinical conclusions [4].

Recent studies on the visual representation of quantitative MRI have highlighted the importance of adapting color LUTs to human perception across various techniques, including perfusion data [19, 20]. However, these studies relied on qualitative assessments rather than experimental trials and lacked a quantitative analysis of the color LUTs most commonly used in clinical practice. Furthermore, by evaluating multiple modalities through a generalized framework, these findings may fail to optimize color LUTs for the specific diagnostic tasks of perfusion data.

To the best of current knowledge, no research has been published specifically examining color LUT schemes for brain perfusion maps derived from DSC-MRI. While there has been some analysis of colorization techniques in myocardial perfusion imaging [21], particularly those involving nuclear medicine tomographic images, these do not directly apply to DSC-MRI data. Furthermore, there are limited studies offering an analysis of the applicability of color LUT schemes in the context of images derived from patient data.

Therefore, *the object of this research* is color lookup table schemes that are most commonly used to visualize perfusion maps in the scope of assessment of brain hemodynamic parameters.

The aim of this research is to assess the most commonly used color LUT schemes for perfusion map visualization by analyzing different quantitative metrics and perceptual characteristics.

To accomplish the aim, the following objectives have been set:

– conduct a direct assessment of the color LUT schemes to analyze the uniformity of color transitions and perceptual changes between neighboring levels;

– evaluate the performance of the color LUT schemes using patient-derived perfusion data by computing quantitative metrics and correlating local grayscale intensity differences with their corresponding perceptual differences in color;

– integrate the results from both assessments to determine key performance indicators and evaluate their impact on the overall effectiveness of the color LUT schemes.

2. Materials and Methods

To evaluate the effectiveness of the color LUT schemes, a comprehensive analysis was conducted that combined direct assessment of the schemes and assessment using actual perfusion map images derived from patient data.

The research used T2*-weighted perfusion magnetic resonance imaging data obtained from the TCGA Research Network [22] during the Glioblastoma Multiform research. BV, BF, and MTT perfusion maps were used from the research [23] and were initially obtained using NordicICE software with its FDA-approved DSC T2* perfusion module (NordicNeuroLab AS, Norway).

To account for the possibility that background in perfusion images may affect the analysis results, binary masks were used to segment the brain from non-brain tissues. All binary masks were previously obtained according to [24, 25] and aligned with the regions of interest (ROIs) for perfusion analysis according to [23]. With their help, only pixels corresponding to the brain perfusion ROI were analyzed; all other pixels were excluded from the analyses (in the perfusion maps, such pixels are usually marked in black).

In this research, nine color LUT schemes (Table 1) from well-known medical equipment manufacturers are analyzed. They are widely used to overlay the corresponding colors onto perfusion maps [26], making the affected areas of the organs visible. Additionally, the *ASIST* color LUT scheme, which was explicitly designed by the Acute Stroke Imaging Standardization Group – Japan (ASIST-Japan) to colorize perfusion parameters in CT and MRI [27], is analyzed.

Table 1

Color LUT schemes used in the research

Color LUT scheme	Visualization
GE-Rainbow	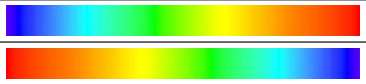
GE-Inv-Rainbow	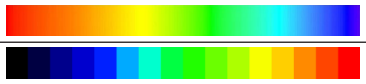
Hitachi-Block	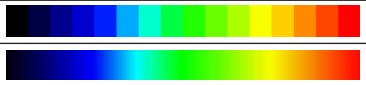
Hitachi-Palette	
Siemens-CT	
Siemens-MR	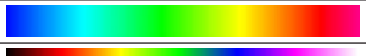
Terarecon	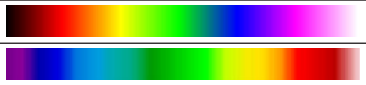
Toshiba-MR	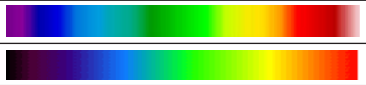
Toshiba-CT	
ASIST	

Each LUT scheme was constructed as a numerical array of RGB triplets. A fixed resolution of 256 equidistant points was enforced for every LUT to align with the 8-bit depth of the greyscale output used for perfusion maps visualization on a monitor. This approach ensures that every grayscale intensity value maps to a unique color coordinate without interpolation artifacts, allowing for a precise pixel-wise comparison of perceptual characteristics across different manufacturer schemes.

Applying the color LUTs yielded a series of variants of the same perfusion map, each with a different color interpretation. All obtained images were stored separately for further analysis.

The perfusion image processing software was in-house developed to provide color modeling by applying the LUT scheme and to assess the results comprehensively. The program was created using Python 3.13.3. Visual Studio Code 1.104.2 was used to develop the software application. The NumPy 1.26.4 library was used to work with arrays, the PyDicom 2.4.4 library to work with medical images in DICOM format, and the PyOpenGL 3.1.7 library for visualization.

To provide a direct assessment of the color LUT schemes, the impact of colors in neighboring levels across each of the analyzed schemes was examined. The colors that formed the LUT scheme arrays were converted from RGB values to the CIELAB color space, using an RGB-to-LAB conversion procedure [28]. The perceptually uniform CIELAB color space, also referred to as $L^*a^*b^*$, was used to provide a consistent relationship between numerical color differences and their actual visual appearance. In the RGB space, identical changes in channel values do not correspond to consistent perceived differences. In contrast, CIELAB represents color through three components: L^* for lightness, a^* for the green-to-red axis, and b^* for the blue-to-yellow axis. This makes it possible to analyze colors in a manner aligned with human visual perception and to more accurately assess distinctions among shades and the uniformity of transitions within a palette [10, 14].

The impact of colors across neighboring levels in the LUT schemes was analyzed using three components.

The first component relies on the analysis of a three-dimensional color path across the LUT scheme in the CIELAB color space. Smoothness of such plots reflects a consistent mapping of intensities to perceptual colors during the transition from greyscale to color representation [28]. In other words, it indicates a stable, well-balanced scheme by assessing perceptual deltas between colors across the schemes.

The second component stands for the analysis of individual values L^*, a^*, and b^* profiles across the LUT scheme. Such plots reveal how the absolute value of lightness and chromatic directions change in the CIELAB color space. So, the smoothness of such plots indicates uniform color transitions and preserved contrast. In contrast, abrupt changes reveal distortions such as loss of detail in mid-tones or oversaturation of specific channels.

To evaluate the uniformity of color transitions in the analyzed LUT schemes, local curvatures and sudden shifts in the plots mentioned above were assessed. This was accomplished by determining the color transition velocity (the discrete first derivative of a sequence of color coordinates in the schemes) and the color transition acceleration (the discrete second derivative). In this research, the color transition velocity represents the rate of color change between neighboring levels in the LUT scheme. Meanwhile, the color transition acceleration identifies fluctuations in that rate, highlighting non-linear patterns in the color change scheme.

The third component of color impact analysis in the LUT schemes is to compute and visualize a distance metric in Euclidean space between each possible color pair in the scheme. Such an analysis for each LUT scheme results in a matrix structured as a heatmap of perceptual distances, where the shade of gray at the specified row-column intersection represents the distance (i. e., higher matrix values yield brighter pixel intensities in the heatmap image). Irregular visual patterns on heatmaps, such as locally bright bands or dark zones, may indicate non-uniformity in the color distribution. The perceptual distance metric ΔE between two colors is quantified as

$$\Delta E = \sqrt{\left(L_2^* - L_1^*\right)^2 + \left(a_2^* - a_1^*\right)^2 + \left(b_2^* - b_1^*\right)^2}, \quad (1)$$

where L^*, a^*, and b^* – color coordinates in the CIELAB space.

To assess the color LUT schemes using actual perfusion map images derived from patient data, several quantitative metrics were computed. Additionally, local perceptual differences in color were compared with underlying intensity differences in perfusion map data.

The following metrics, which quantify image similarity before and after colorization of perfusion maps, were analyzed.

Root mean square error (RMSE) quantifies the difference in each pixel before and after processing [29]. The lower its value, the greater the similarity between images. This metric is used exclusively for grayscale images. It is simple to calculate, but it does not account for the structural features of images.

Peak signal-to-noise ratio (PSNR) is an indicator that determines the level of signal relative to noise in an image [29]. The higher its value, the less information loss. Like RMSE, this metric is used for grayscale images. It is simple and easy to interpret, but it does not account for the structural features of images and depends on the noise level.

Structural similarity index measure (SSIM) estimates structural changes in an image rather than deviations of individual pixels [30]. Its value ranges from –1 to 1, where 1 indicates maximum similarity between images. SSIM accounts for structural features of images and correlates with human perception.

Feature similarity index measure (FSIM) uses feature detection to evaluate image quality or similarity, relying on phase convergence and gradient magnitude. It was developed to assess the similarity of structural features between restored and original images [31]. The index value ranges from 0 to 1, where 1 indicates complete identity of the images.

Information-theoretic-based statistic similarity measure (ISSM) applies information theory to analyze image similarity by evaluating their mutual information and entropy [32]. This metric accounts for the statistical characteristics of images. The ISSM value ranges from 0 to 1, where 0 indicates no similarity between the compared images, and 1 indicates perfect similarity (i. e., the images are identical in terms of statistical characteristics).

Signal-to-reconstruction error (SRE) determines the level of error relative to the signal strength [33]. SRE is a measure of how accurately an algorithm reproduces the original pixel intensities after processing, conversion, or compression. A higher SRE value indicates better image quality and less processing-induced distortion. SRE is sensitive to noise and does not account for spatial relationships between neighboring pixels.

Spectral angle mapper (SAM) measures spectral similarity between image pixels and known reference spectra by treating them as vectors in a space, which dimension corresponds to the number of bands [34]. The smaller value, the closer the match to the reference spectra. The main advantage of SAM is its ability to account for the spectral characteristics of images.

Universal image quality (UIQ) measures the overall quality of an image by analyzing parameters such as file size, contrast, brightness, etc. [35]. The UIQ value ranges from –1 to 1, where 1 indicates identical images, 0 indicates no correlation between analyzed images, and negative values may occur in cases of severe distortion or if the image structure is inverted.

Since RMSE and PSNR work with grayscale images, to apply them, the colored perfusion maps were converted to grayscale using a specific algorithm. The process consists of three main steps: first, obtain the red, green, and blue channel values for each pixel; second, apply a mathematical formula to combine the red, green, and blue channels into a single grayscale value; and third, replace the original values of the red, green, and blue channels with the resulting grayscale value.

ISSN-L 2664-9969; E-ISSN 2706-5448

Usually, the second step involves averaging the red, green, and blue channels. However, to take into account the peculiarities of color perception by the human eye, which is sensitive to green and blue colors, different weights were used for the channels

$$Grayscale = 0.299 \cdot R + 0.587 \cdot G + 0.114 \cdot B, \quad (2)$$

where *Grayscale* – the grayscale value for a pixel in a grayscale image; *R*, *G*, and *B* – the values of the red, green, and blue channels of the corresponding pixel in a color image [4].

To assess how consistently each LUT scheme reflects variations in the underlying greyscale data, the relationship between local intensity differences in greyscale perfusion maps was analyzed. These differences were then compared to the corresponding color perceptual differences in CIELAB space after colorizing the perfusion maps. The sample slice with the largest pixel count in the brain segment was selected to determine three perfusion maps (i. e., BV, BF, and MTT) for this assessment.

For every pair of neighboring pixels in the perfusion map image, the absolute difference in the original scalar values (ΔI) was computed together with the perceptual color difference (ΔE) between the two corresponding CIELAB colors. This procedure was applied separately in the horizontal and vertical directions. The result was two large sets of ΔI – ΔE pairs for each LUT that together capture the full range of local transitions present in the sample perfusion map images. Based on these data, a linear relationship was then estimated between intensity differences and color perceptual differences. For each direction, a linear regression model without an intercept was fitted to predict ΔE from ΔI, describing how proportionally a given LUT scheme reflects local intensity changes into perceptual changes in color. The quality of this correspondence was quantified using the coefficient of determination R^2 derived from the fitted regression. Therefore, perceptually better color LUT schemes produce scatter plots in which the ΔI – ΔE pairs form a diffuse cloud tightly aligned with the regression line, resulting in higher slopes and R^2 values. Specifically, higher slopes correspond to increased sensitivity between colors, while high R^2 values indicate greater perceptual uniformity.

3. Results and Discussion

3.1. Direct assessment of the color LUT schemes

The perceptual assessment results of the impact of colors across neighboring levels in the LUT schemes are summarized in three figures for each analyzed component separately. Specifically, Fig. 1 shows the three-dimensional color path in the CIELAB space, Fig. 2 displays individual L^*, a^*, and b^* profiles, and Fig. 3 presents heatmaps of perceptual distances between each possible color pair.

Visual inspection of the plots in Fig. 1 suggests that *GE-Rainbow* and *GE-Inv-Rainbow* cases are smoother and exhibit fewer abrupt changes, while the results in Fig. 2 also identify *Siemens-MR*, *Terarecon*, and *ASIST* cases. At the same time, the assessment of Color Transition Velocity and Color Transition Acceleration across all cases (Table 2) indicates *ASIST* and *Siemens-MR* as best-performing schemes.

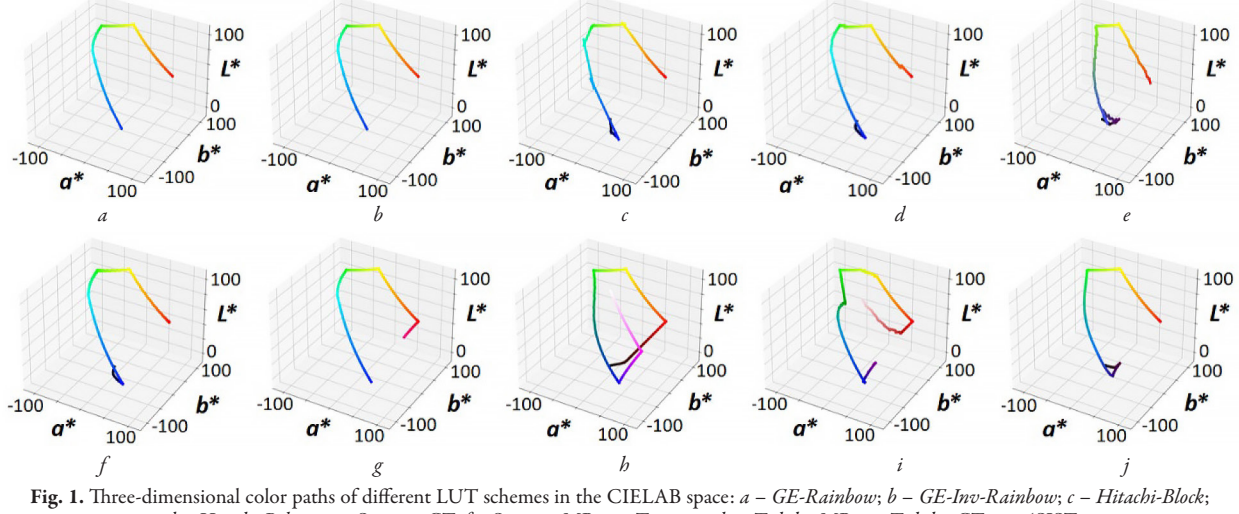

Fig. 1. Three-dimensional color paths of different LUT schemes in the CIELAB space: *a* – *GE-Rainbow*; *b* – *GE-Inv-Rainbow*; *c* – *Hitachi-Block*; *d* – *Hitachi-Palette*; *e* – *Siemens-CT*; *f* – *Siemens-MR*; *g* – *Terarecon*; *h* – *Toshiba-MR*; *i* – *Toshiba-CT*; *j* – *ASIST*

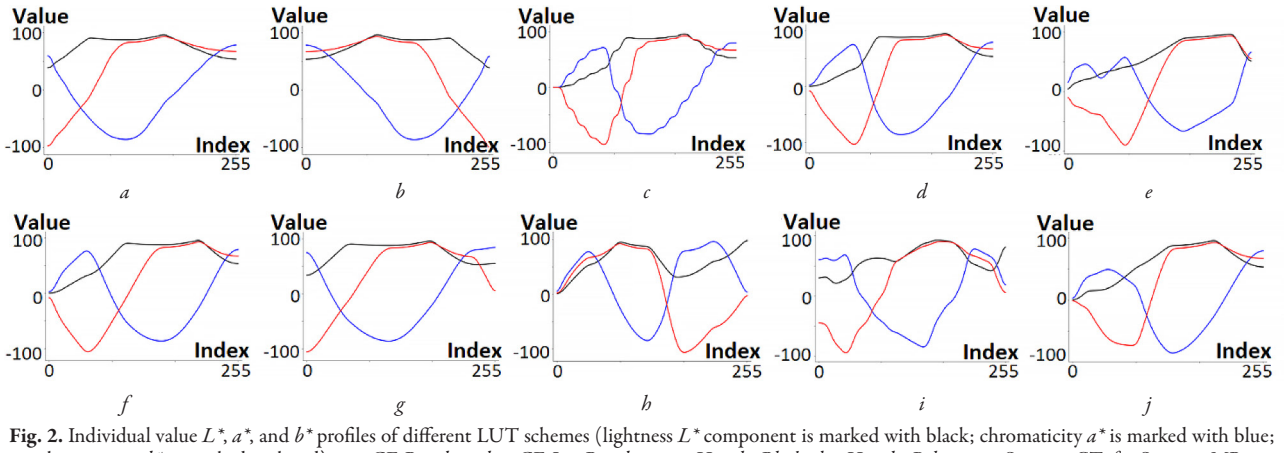

Fig. 2. Individual value L^*, a^*, and b^* profiles of different LUT schemes (lightness L^* component is marked with black; chromaticity a^* is marked with blue; chromaticity b^* is marked with red): *a* – *GE-Rainbow*; *b* – *GE-Inv-Rainbow*; *c* – *Hitachi-Block*; *d* – *Hitachi-Palette*; *e* – *Siemens-CT*; *f* – *Siemens-MR*; *g* – *Terarecon*; *h* – *Toshiba-MR*; *i* – *Toshiba-CT*; *j* – *ASIST*

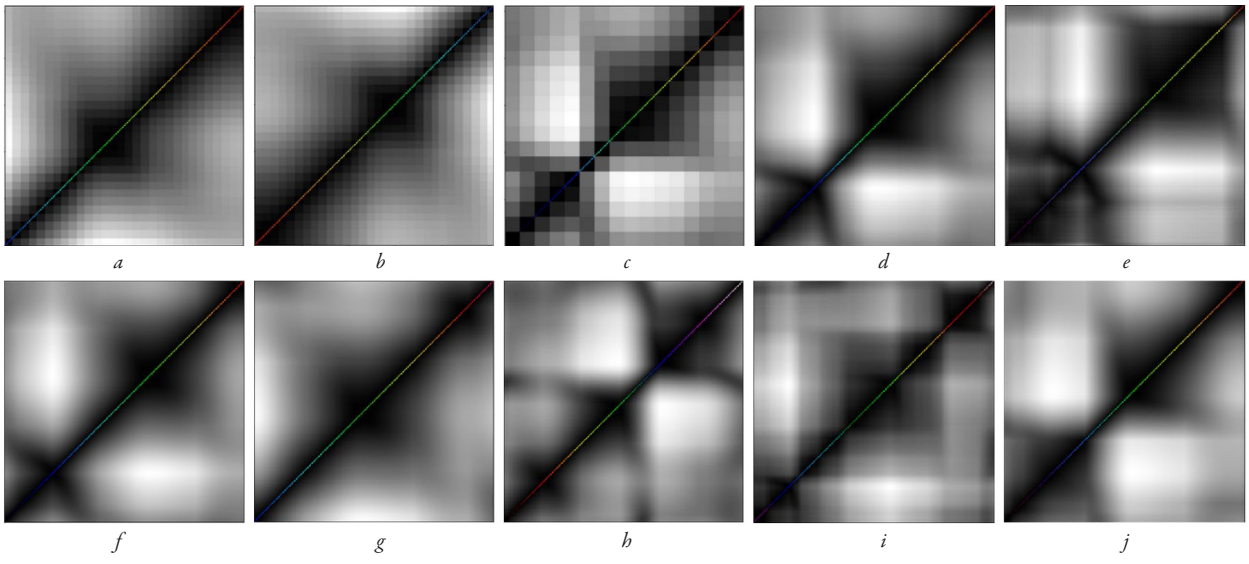

Fig. 3. Heatmaps of perceptual distances between each possible color pair in the different LUT schemes: *a* – *GE-Rainbow*; *b* – *GE-Inv-Rainbow*; *c* – *Hitachi-Block*; *d* – *Hitachi-Palette*; *e* – *Siemens-CT*; *f* – *Siemens-MR*; *g* – *Terarecon*; *h* – *Toshiba-MR*; *i* – *Toshiba-CT*; *j* – *ASIST*

Also, it can be observed that a block-structured scheme, such as *Hitachi-Block*, exhibits notable issues of abrupt chromatic oscillations. These limitations may lead to visual artifacts, in which minor variations in perfusion values are either overstated or understated, thereby compromising diagnostic reliability.

Table 2

Quantitative comparisons of color transitions in the color LUT schemes

Color LUT scheme	Color transition velocity				Color transition acceleration, 3D path
	3D path	L^*	a^*	b^*	
GE-Rainbow	2.6070	1.3537	3.2830	2.7547	2.6224
GE-Inv-Rainbow	2.6158	1.3537	3.2830	2.7547	2.6258
Hitachi-Block	6.3664	3.0635	7.6911	7.2483	4.5310
Hitachi-Palette	1.4170	0.6974	1.4844	1.6604	1.9728
Siemens-CT	2.1254	1.1755	2.6376	2.1712	4.4940
Siemens-MR	**0.9129**	0.4751	0.9014	**0.9625**	0.5409
Terarecon	1.0219	0.5127	1.0258	1.1846	1.2475
Toshiba-MR	1.5948	0.7509	1.7608	1.8169	1.8731
Toshiba-CT	1.4957	**1.0151**	**1.7614**	1.4976	**2.0554**
ASIST	0.9639	0.3643	0.8886	1.2329	0.1162

Note: the results of best and second-best performing schemes are marked in bold and underlined, respectively

Analyzing the results in Fig. 3, which show heatmaps of perceptual distances between each possible color pair in the LUT schemes, it is evident that the *Hitachi-Palette, Siemens-MR, Terarecon*, and *ASIST* cases exhibit the most consistent and uniform patterns. In contrast, block-structured *Hitachi-Block* and *Toshiba-CT* schemes exhibit localized anomalies (i. e., sharply defined bright and dark regions, multiple discontinuity zones, and fragmented diagonal patterns).

3.2. Assessment of the color LUT schemes using perfusion maps derived from patient data

Table 3 presents the outcomes of quantitative metrics used to evaluate color LUT schemes, based on actual perfusion map images derived from patient data. Since the number of metric values to be compared in the scope of the LUT scheme quantitative assessment was significant, thresholds for metrics were introduced. Rather than applying arbitrary fixed values, thresholds were statistically determined using quartile-based cut-offs derived from the aggregate distribution of all processed perfusion maps across all analyzed color LUT schemes. For metrics where higher values indicate superior quality (e. g., PSNR, SSIM, FSIM, ISSM, SRE, and UIQ), the threshold was set to the third quartile (Q3). Conversely, for error-based metrics where lower values represent better performance (e. g., RMSE and SAM), the threshold was established at the first quartile (Q1) to represent the best-performing 25% of the data. Namely: RMSE – 0.0044, PSNR – 44.46, SSIM – 0.8951, FSIM – 0.5901, ISSM – 0.6771, SRE – 26.274, SAM – 76.706, UIQ – 0.0095. Subsequently, a success rate was calculated for each color LUT scheme, defined as the percentage of cases in perfusion map images that successfully met these statistically derived criteria.

Table 3 indicates that among all schemes, *ASIST* and *Siemens-MR* appeared to be the most effective for the perfusion maps used in this research, maintaining both accuracy (RMSE and PSNR) and visual similarity (SSIM and UIQ). It should be noted that some LUT schemes, in particular *Hitachi-Palette*, exhibit relatively high values on several quantitative indicators. At the same time, *GE-Rainbow* and *GE-Inv-Rainbow* are significantly inferior to other schemes, making them less suitable for tasks where image quality is critical.

Table 3

Quantitative assessment of the color LUT schemes based on actual perfusion map images derived from patient data

Color LUT scheme	Quantitative metrics, percentage of cases exceeding the threshold							
	RMSE	PSNR	SSIM	FSIM	ISSM	SRE	SAM	UIQ
GE-Rainbow	0	0	2.22	20.56	41.11	1.67	26.67	0
GE-Inv-Rainbow	4.44	2.22	3.89	24.44	36.11	17.78	6.11	0
Hitachi-Block	40	30	33.89	28.33	***52.78***	35	0.56	26.11
Hitachi-Palette	41.67	45	**56.67**	21.11	0.56	54.44	**100**	40.56
Siemens-CT	26.11	26.67	12.78	**35.56**	11.67	10	8.89	51.67
Siemens-MR	30	27.78	**56.67**	34.44	25.56	**55.56**	50.56	47.22
Terarecon	10	20	2.22	20	24.44	3.33	19.44	0
Toshiba-CT	4.44	1.11	9.44	7.78	22.22	0.56	5.56	10
Toshiba-MR	46.11	47.22	25.56	24.44	30	30.56	0.56	20
ASIST	**47.22**	**50**	46.67	33.33	5.56	41.11	31.67	**54.44**

Note: the results of best and second-best performing schemes are marked in bold and underlined, respectively

ISSN-L 2664-9969; E-ISSN 2706-5448

The ISSM metric focuses on evaluating the preservation of structural differences between image regions. For this reason, block LUTs performed best on this metric, as discrete color changes enhance local contrast transitions. However, such enhancement can lead to a loss of smooth transitions and distortion of the actual intensity distribution, which is crucial for accurate clinical interpretation. Therefore, using only the ISSM metric to evaluate the quality of LUT schemes may be insufficient and needs to be supplemented with other metrics.

To compare local perceptual differences in color and underlying intensity differences in perfusion map data, the linear regression model without an intercept was applied to the sample perfusion map images. Table 4 summarizes the results of linear regression analysis.

Table 4

Results of regression analysis for each color LUT scheme applied to the sample perfusion map images

Color LUT scheme	Linear regression equation, $y = \beta x$; R^2 coefficient of determination		
	BF	BV	MTT
GE-Rainbow	$y = 35.8x$; $R^2 = 0.72$	$y = 36.3x$; $R^2 = 0.72$	$y = 39.1x$; $R^2 = 0.70$
GE-Inv-Rainbow	$y = 20.7x$; $R^2 = 0.70$	$y = 20.2x$; $R^2 = 0.70$	$y = 21.2x$; $R^2 = 0.81$
Hitachi-Block	$y = 38.3x$; $R^2 = 0.76$	$y = 37.4x$; $R^2 = 0.75$	$y = 43.7x$; $R^2 = 0.72$
Hitachi-Palette	$y = 46.9x$; $R^2 = 0.77$	$y = 45.9x$; $R^2 = 0.77$	$\underline{y = 53.3x}$; $R^2 = 0.73$
Siemens-CT	$y = 42.1x$; $R^2 = 0.82$	$y = 41.5x$; $R^2 = 0.82$	$y = 41.6x$; $\mathbf{R^2 = 0.86}$
Siemens-MR	$\underline{y = 47.9x}$; $\underline{R^2 = 0.84}$	$\underline{y = 46.9x}$; $\mathbf{R^2 = 0.84}$	$y = 53.2x$; $\underline{R^2 = 0.85}$
Terarecon	$y = 46.3x$; $R^2 = 0.82$	$y = 45.3x$; $R^2 = 0.81$	$y = 47.3x$; $R^2 = 0.84$
Toshiba-MR	$\mathbf{y = 57.8x}$; $R^2 = 0.78$	$\mathbf{y = 55.8x}$; $R^2 = 0.75$	$\mathbf{y = 59.3x}$; $R^2 = 0.73$
Toshiba-CT	$y = 43.9x$; $R^2 = 0.81$	$y = 42.4x$; $R^2 = 0.80$	$y = 45.2x$; $R^2 = 0.83$
ASIST	$y = 46.7x$; $\mathbf{R^2 = 0.85}$	$y = 45.7x$; $\underline{R^2 = 0.83}$	$y = 48.8x$; $\underline{R^2 = 0.85}$

Note: the results of best and second-best performing schemes are marked in bold and underlined, respectively

From the results of linear regression analysis, it was found that *Siemens-CT*, *Siemens-MR*, and *ASIST* schemes consistently demonstrate the highest linearity across all perfusion maps ($R^2 > 0.84$), ensuring a predictable perceptual response. Meanwhile, the *Toshiba-MR* scheme exhibits the highest sensitivity, characterized by the steepest slope coefficients ($\beta > 55$), enabling effective differentiation of subtle signal changes.

3.3. Key performance indicators and their impact on the overall effectiveness of the color LUT schemes

Based on the results from both assessments, it is evident that evaluating the overall effectiveness of color LUT schemes requires a multi-dimensional approach rather than a single-metric analysis. The results of this research demonstrate that certain metrics are more sensitive than others to the specific perceptual irregularities and mapping inconsistencies found in perfusion map colorization.

Specifically, color transition velocity was established as a primary indicator for the direct assessment of color transitions between neighboring levels. The results revealed that LUT schemes with high velocity fluctuations in these transitions corresponded directly to visible irregularities in the clinical maps. The findings indicated that schemes with minimal velocity fluctuations in these transitions corresponded to more stable color changes and fewer visual inconsistencies within the clinical perfusion maps. The performance of the RMSE, PSNR, SSIM, and UIQ metrics helped identify deviations in signal integrity. These metrics provided effective indicators for the quantitative assessment of image similarity before and after colorization of actual perfusion maps. In particular, SSIM and UIQ reflected the preservation of structural details, which is not captured by pixel-wise calculations alone. The linear regression analysis between local perceptual differences in color and underlying intensity differences in perfusion map data acted as one more key performance indicator for assessing LUT schemes. The strong correlation values obtained for top-performing schemes indicate that this metric is capable to quantify of how consistently the LUT scheme reflects variations in the underlying greyscale data.

The results showed that the selection of the color LUT scheme plays an essential role in maintaining perfusion map integrity, both in terms of intensity preservation and in the representation of structural features. The *ASIST*, *Hitachi-Palette*, *Siemens-MR* and *Toshiba-MR* schemes demonstrated the most stable and consistent performance across most quantitative and perceptual criteria. In contrast, spectral rainbow LUTs, in particular *Siemens-CT*, *Terarecon,* and *Toshiba-CT*, were found to be less effective, potentially introducing distortions in visual information and resulting in the omission of critical diagnostic details. Therefore, the results confirm the need for a comprehensive approach to evaluating color LUT schemes and justify the advantages of perceptually optimized LUTs for visualizing perfusion data in both scientific and clinical contexts.

The findings from this research can be directly use in clinical applications for enhancing the visualization of hemodynamic parameters (CBV, CBF, and MTT). Furthermore, they facilitate the standardization of imaging workflows and offer a validated benchmark for developing algorithms used to calculate perfusion maps.

3.4. Research limitations and directions for its development

This research has several limitations that should be considered when interpreting the results.

Firstly, DSC-MRI perfusion data from only glioblastoma patients were used.

Second, the research does not include subjective assessment from human observers. While conducted analysis provides a standardized benchmark for assessment of different color LUT schemes, it cannot fully account for the complex ways of physicians perceiving perfusion maps data. These perceptions can affect how they understand the information and make their treatment decisions.

Further research could expand the dataset to include perfusion maps from not only glioblastoma patients but also those with various other pathologies. This would allow for a more comprehensive evaluation of the results and assess the effectiveness of color LUT schemes across a wider range of clinical scenarios. Additionally, further research could explore the psychophysical mechanisms of color perception. In particular, conducting multi-observer research could allow for an assessment of how color LUT schemes perform across a variety of physicians, accounting for individual variability in human perception.

4. Conclusions

1. A direct assessment of the color LUT schemes revealed significant variations in perceptual stability. The analysis of color transitions between neighboring levels showed that while some schemes maintained consistent perceptual steps, others exhibited notable issues of abrupt chromatic oscillations. Specifically, the *ASIST* and *Siemens-MR* schemes exhibited the highest values for color transition velocity, recording 0.9129 (optimal) and 0.9639, respectively. regarding color transition acceleration, the *ASIST* scheme demonstrated a high performance value of 0.5409, while the *Siemens-MR* scheme achieved an optimal value of 0.1162.

2. Quantitative evaluation using patient-derived perfusion data revealed that LUT selection significantly impacts the structural integrity

of the visualized data. The *ASIST* and *Siemens-MR* schemes appeared to be the most effective for the perfusion maps used in this research. The *ASIST* scheme achieved optimal metrics with a RMSE of 47.22, PSNR of 50, and UIQ of 54.44. It also ranked second in SSIM with a value of 46.67. On the other hand, the *Siemens-MR* scheme excelled in SSIM with a score of 56.67 and SRE of 55.56, while attaining the second-best results in FSIM at 34.44 and SAM at 50.56. By correlating local grayscale intensity differences with their corresponding perceptual differences in color, it was found that *Siemens-CT*, *Siemens-MR*, and *ASIST* schemes achieved the highest linearity across all perfusion maps ($R^2 > 0.84$). This indicates that underlying intensity differences were accurately represented by corresponding color changes, ensuring a predictable perceptual response. At the same time, the *Toshiba-MR* scheme demonstrated superior sensitivity, marked by slope coefficients ($\beta > 55$) that are notably steep. This characteristic allows for precise differentiation of subtle signal changes.

3. By integrating the results from both direct and image-based assessments, key performance indicators can be established to evaluate overall effectiveness. The results demonstrate that color transition velocity, RMSE and PSNR metrics for accuracy, SSIM and UIQ metrics for visual similarity are primary drivers of color LUTs effectiveness. Additionally, significant insights can be derived from conducting linear regression analysis between local intensity differences and perceptual differences in color. Based on these, the *ASIST* and *Siemens-MR* scheme was identified as the most effective for visualization of perfusion maps derived from DSC-MRI.

Conflict of interest

The authors declare that they have no conflict of interest in relation to this research, whether financial, personal, authorship or otherwise, that could affect the research and its results presented in this paper.

Financing

The research was performed without financial support.

Data availability

Manuscript has associated data in a data repository.

Use of artificial intelligence

Grammarly: AI Writing and Grammar Checker App, Version 8.934.0, was used to check the grammar in this paper.

Each suggested grammar improvement was checked for applicability and, if applicable, for content correctness.

The results do not affect the research conclusions.

Authors' contributions

Svitlana Alkhimova: Conceptualization, Data curation, Investigation, Project administration, Supervision, Validation, Visualization, Writing – review and editing; ***Viktoriia Sorokina***: Data curation, Formal analysis, Investigation, Software, Visualization, Writing – original draft; ***Illia Kabala***: Data curation, Formal analysis, Investigation, Software, Visualization, Writing – original draft.

References

1. Putowski, Z., Bakker, J., Kattan, E., Hernández, G., Ait-Oufella, H., Szczeklik, W., Guerci, P. (2025). Tissue perfusion as the ultimate target of hemodynamic interventions in the perioperative period. *Journal of Clinical Anesthesia, 107,* 112009. https://doi.org/10.1016/j.jclinane.2025.112009
2. Lipiński, S. (2024). Creation of a Simulated Sequence of Dynamic Susceptibility Contrast–Magnetic Resonance Imaging Brain Scans as a Tool to Verify the Quality of Methods for Diagnosing Diseases Affecting Brain Tissue Perfusion. *Computation, 12 (3),* 54. https://doi.org/10.3390/computation12030054
3. Sobhan, R., Gkogkou, P., Johnson, G., Cameron, D. (2023). *Model-based deconvolution for DSC-MRI: A comparison of accuracy, precision, and computational complexity of parametric transit time distributions.* https://doi.org/10.1101/2023.02.12.528216
4. Sorokina, V. V., Alkhimova, S. M. (2024). Analiz zastosuvannia tablyts vidpovidnosti koloriv dlia vizualizatsii danykh perfuziinykh kart. *World Ways and Methods of Improving Outdated Theories and Trends*, 380–385. Available at: https://isg-konf.com/world-ways-and-methods-of-improving-outdated-theories-and-trends/
5. Căiniceanu, A.-M.-A., Alexa, F. (2025). Application of Color Theory in Graphic Design. *2025 18th International Conference on Engineering of Modern Electric Systems (EMES).* IEEE 1–6. https://doi.org/10.1109/emes65692.2025.11045619
6. Furmanová, K., Kozlíková, B., Höllt, T., Gröller, M. E., Preim, B., Raidou, R. G. (2025). *BioMedical Visualization. Synthesis Lectures on Visualization.* Springer Nature Switzerland. https://doi.org/10.1007/978-3-031-66789-3
7. Preim, B., Oeltze, S., Mlejnek, M., Groeller, E., Hennemuth, A., Behrens, S. (2009). Survey of the Visual Exploration and Analysis of Perfusion Data. *IEEE Transactions on Visualization and Computer Graphics, 15 (2),* 205–220. https://doi.org/10.1109/tvcg.2008.95
8. Garrison, L. A., Kolesar, I., Viola, I., Hauser, H., Bruckner, S. (2022). Trends & Opportunities in Visualization for Physiology: A Multiscale Overview. *Computer Graphics Forum, 41 (3),* 609–643. https://doi.org/10.1111/cgf.14575
9. Crameri, F., Shephard, G. E., Heron, P. J. (2020). The misuse of colour in science communication. *Nature Communications, 11 (1).* https://doi.org/10.1038/s41467-020-19160-7
10. Moreland, K. (2016). Why We Use Bad Color Maps and What You Can Do About It. *Electronic Imaging, 28 (16),* 1–6. https://doi.org/10.2352/issn.2470-1173.2016.16.hvei-133
11. Reda, K. (2023). Rainbow Colormaps: What are They Good and Bad for? *IEEE Transactions on Visualization and Computer Graphics, 29 (12),* 5496–5510. https://doi.org/10.1109/tvcg.2022.3214771
12. Liu, Y., Heer, J. (2018). Somewhere Over the Rainbow. *Proceedings of the 2018 CHI Conference on Human Factors in Computing Systems,* 1–12. https://doi.org/10.1145/3173574.3174172
13. Stoelzle, M., Stein, L. (2021). Rainbow color map distorts and misleads research in hydrology – guidance for better visualizations and science communication. *Hydrology and Earth System Sciences, 25 (8),* 4549–4565. https://doi.org/10.5194/hess-25-4549-2021
14. Silva, S., Sousa Santos, B., Madeira, J. (2011). Using color in visualization: A survey. *Computers & Graphics, 35 (2),* 320–333. https://doi.org/10.1016/j.cag.2010.11.015
15. Sibrel, S. C., Rathore, R., Lessard, L., Schloss, K. B. (2020). The relation between color and spatial structure for interpreting colormap data visualizations. *Journal of Vision, 20 (12),* 7. https://doi.org/10.1167/jov.20.12.7
16. Zabala-Travers, S., Choi, M., Cheng, W.-C., Badano, A. (2015). Effect of color visualization and display hardware on the visual assessment of pseudocolor medical images. *Medical Physics, 42 (6),* 2942–2954. https://doi.org/10.1118/1.4921125
17. Nuñez, J. R., Anderton, C. R., Renslow, R. S. (2018). Optimizing colormaps with consideration for color vision deficiency to enable accurate interpretation of scientific data. *PLOS ONE, 13 (7),* e0199239. https://doi.org/10.1371/journal.pone.0199239
18. Ware, C., Turton, T. L., Bujack, R., Samsel, F., Shrivastava, P., Rogers, D. H. (2019). Measuring and Modeling the Feature Detection Threshold Functions of Colormaps. *IEEE Transactions on Visualization and Computer Graphics, 25 (9),* 2777–2790. https://doi.org/10.1109/tvcg.2018.2855742
19. Sollmann, N., Fuderer, M., Crameri, F., Weingärtner, S., Baeßler, B., Gulani, V. et al. (2024). Color Maps: Facilitating the Clinical Impact of Quantitative MRI. *Journal of Magnetic Resonance Imaging, 61 (4),* 1572–1579. https://doi.org/10.1002/jmri.29573
20. deSouza, N. M., Fuderer, M., Sollmann, N., Wichtmann, B. D., Golay, X. (2025). Colour map displays. *Insights into Imaging, 16 (1).* https://doi.org/10.1186/s13244-025-01970-2
21. Qutbi, M. (2024). Quantitative Performance Evaluation of Commonly Used Colormaps for Image Display in Myocardial Perfusion Imaging: Analysis based on Perceptual Metrics. *Molecular Imaging and Radionuclide Therapy, 33 (2),* 94–105. https://doi.org/10.4274/mirt.galenos.2024.34711
22. The Cancer Genome Atlas Program (TCGA). *Cancer.gov.* Available at: http://cancergenome.nih.gov/
23. Jain, R., Poisson, L., Narang, J., Gutman, D., Scarpace, L., Hwang, S. N. et al. (2013). Genomic Mapping and Survival Prediction in Glioblastoma: Molecular Subclassification Strengthened by Hemodynamic Imaging Biomarkers. *Radiology, 267 (1),* 212–220. https://doi.org/10.1148/radiol.12120846
24. Alkhimova, S., Krenevych, A. (2019). Brain tissues segmentation on mr perfusion images using CUSUM filter for boundary pixels. *International Journal of Computing, 18 (2),* 127–134. https://doi.org/10.47839/ijc.18.2.1411

ISSN-L 2664-9969; E-ISSN 2706-5448

25. Alkhimova, S. (2019). CUSUM Filter for Brain Segmentation on DSC Perfusion MR Head Scans with Abnormal Brain Anatomy. *Proceedings of the 2019 International Conference on Intelligent Medicine and Image Processing*, 43–47. https://doi.org/10.1145/3332340.3332357

26. Kudo, K., Sasaki, M., Yamada, K., Terae, S., Tha, K. K., Yoshida, Y., Miyasaka, K. (2006). Evaluation and minimization of the difference in MR perfusion maps among software. *Proceedings of the 14th Annual Meeting of ISMRM*, 3558. Available at: https://cds.ismrm.org/protected/06MProceedings/PDFfiles/03558.pdf

27. Kudo, K. (2005). *Acute Stroke Imaging Standardization Group Japan recommended standard LUT (a-LUT) for perfusion color maps.*

28. Schanda, J. (Ed.) (2007). *Colorimetry: understanding the CIE system.* John Wiley & Sons. https://doi.org/10.1002/9780470175637

29. Sara, U., Akter, M., Uddin, M. S. (2019). Image Quality Assessment through FSIM, SSIM, MSE and PSNR – A Comparative Study. *Journal of Computer and Communications, 7 (3)*, 8–18. https://doi.org/10.4236/jcc.2019.73002

30. Sampat, M. P., Zhou Wang, Gupta, S., Bovik, A. C., Markey, M. K. (2009). Complex Wavelet Structural Similarity: A New Image Similarity Index. *IEEE Transactions on Image Processing, 18 (11)*, 2385–2401. https://doi.org/10.1109/tip.2009.2025923

31. Lin Zhang, Lei Zhang, Xuanqin Mou, Zhang, D. (2011). FSIM: A Feature Similarity Index for Image Quality Assessment. *IEEE Transactions on Image Processing, 20 (8)*, 2378–2386. https://doi.org/10.1109/tip.2011.2109730

32. Aljanabi, M. A., Hussain, Z. M., Shnain, N. A. A., Lu, S. F. (2019). Design of a hybrid measure for image similarity: a statistical, algebraic, and information-theoretic approach. *European Journal of Remote Sensing, 52*, 2–15. https://doi.org/10.1080/22797254.2019.1628617

33. Nordio, A., Chiasserini, C.-F., Viterbo, E. (2009). Signal Reconstruction Errors in Jittered Sampling. *IEEE Transactions on Signal Processing, 57 (12)*, 4711–4718. https://doi.org/10.1109/tsp.2009.2027404

34. Yuhas, R. H., Goetz, A. F., Boardman, J. W. (1992). Discrimination among semi-arid landscape endmembers using the spectral angle mapper (SAM) algorithm. *JPL, Summaries of the Third Annual JPL Airborne Geoscience Workshop. Volume 1: AVIRIS Workshop*. Available at: https://ntrs.nasa.gov/citations/19940012193

35. Zhou Wang, Bovik, A. C. (2002). A universal image quality index. *IEEE Signal Processing Letters, 9 (3)*, 81–84. https://doi.org/10.1109/97.995823

✉ ***Svitlana Alkhimova,*** *PhD, Department of Biomedical Cybernetics, National Technical University of Ukraine "Igor Sikorsky Kyiv Polytechnic Institute", Kyiv, Ukraine, e-mail: alkhimova.svitlana@lll.kpi.ua, ORCID: http://orcid.org/0000-0002-9749-7388*

Viktoriia Sorokina, *Department of Biomedical Cybernetics, National Technical University of Ukraine "Igor Sikorsky Kyiv Polytechnic Institute", Kyiv, Ukraine, ORCID: https://orcid.org/0009-0005-8911-9765*

Illia Kabala, *Department of Biomedical Cybernetics, National Technical University of Ukraine "Igor Sikorsky Kyiv Polytechnic Institute", Kyiv, Ukraine, ORCID: https://orcid.org/0009-0006-3450-9472*

✉ *Corresponding author*